

Characterization of the transglutaminase gene family in zebrafish and in vivo analysis of transglutaminase-dependent bone mineralization

Stephanie Deasey · Olga Grichenko ·
Shaojun Du · Maria Nurminskaya

Received: 25 March 2011 / Accepted: 7 June 2011 / Published online: 2 August 2011
© Springer-Verlag 2011

Abstract We have characterized the protein cross-linking enzyme transglutaminase (TGs) genes in zebrafish, *Danio rerio*, based on the analysis of their genomic organization and phylogenetics. Thirteen zebrafish TG genes (zTGs) have been identified, of which 11 show high homology to only 3 mammalian enzymes: *TG1*, *TG2* and *FXIIIa*. No zebrafish homologues were identified for mammalian TGs 3–7. Real-time PCR analysis demonstrated distinct temporal expression profiles for zTGs in larvae and adult fish. Analysis by in situ hybridization revealed restricted expression of zTG2b and zFXIIIa in skeletal elements, resembling expression of their mammalian homologues in osteo-chondrogenic cells. Mammalian TG2 and FXIIIa have been implicated in promoting osteoblast differentiation and bone mineralization in vitro, however, mouse models lacking either gene have no skeletal phenotype likely due to a compensation effect. We show in this study that mineralization of the newly formed vertebrae is significantly reduced in fish grown for 5 days in the presence of TG inhibitor KCC-009 added at 3–5 days post fertilization. This treatment reduces average vertebrae mineralization by 30%, with complete inhibition in some fish, and no effect on the overall growth and vertebrae number. This is the first in vivo demonstration of the crucial requirement for the TG-catalyzed cross-linking activity in bone mineralization.

Keywords Transglutaminase · Inhibitors · Zebrafish · Bone development

Abbreviations

dpf	Days post-fertilization
DMSO	Dimethyl sulfoxide
FXIIIa	Factor thirteen A
hTG	Human transglutaminase
gplTG2	Purified guinea pig liver transglutaminase 2
SL	Standard length
TGs	Transglutaminases
zTGs	Zebrafish transglutaminases

Introduction

The comprehensive identification and understanding of both systemic and local bone anabolic factors is essential for the development of new therapeutic targets to treat bone diseases and fractures. Previous in vitro studies have implicated enzyme transglutaminases (TGs) in osteoblast differentiation and deposition of mineralized matrix. TGs (R-glutaminylpeptide: amine- γ -glutamyl transferases, EC 2.3.2.13) are multifunctional Ca^{2+} dependent proteins that are crucial for the formation of ϵ -(γ -glutamyl)-lysine-protein cross-links (Lorand and Graham 2003). In mammals, the family of catalytically active TG is comprised of eight proteins, TGs1–7 and FXIIIa, with most of the mammalian TGs being expressed in a tissue-specific manner.

Two mammalian TGs, TG2 and FXIIIa, are up-regulated in the osteo-chondrogenic lineage (Aeschlimann et al. 1993; Nurminskaya and Linsenmayer 1996; Borge et al. 1996; Rosenthal et al. 1997; Nurminskaya and Linsenmayer 2002; Summey et al. 2002; Al-Jallad et al. 2005). Both enzymes are expressed in pre-hypertrophic and hypertrophic

S. Deasey · O. Grichenko · S. Du · M. Nurminskaya (✉)
Department of Biochemistry and Molecular Biology, University
of Maryland School of Medicine, Baltimore, MD 21201, USA
e-mail: mnurminskaya@som.umaryland.edu

chondrocytes of the growth plate and in the “borderline chondrocytes” that are localized to the lateral edges of the growth plate (Nurminskaya and Kaartinen 2006). These “borderline chondrocytes” are thought to regulate the formation of the bony collar (Bianco et al. 1998), suggesting that extracellular chondrocyte-derived TGs may regulate osteoblast differentiation in the periosteal bone. This hypothesis has been confirmed in vitro by the ability of TG2 and FXIIIa to promote differentiation in osteoblasts (Nurminskaya et al. 2003; Becker et al. 2008), and osteoblast-like transformation in vascular smooth muscle cells (Faverman et al. 2008). Nevertheless, despite the in vitro evidence, genetic ablation of either enzyme has no effect on skeletal phenotype in mouse models (Nanda et al. 2001; Lauer et al. 2002; Koseki-Kuno et al. 2003). A plausible explanation for the discrepancy between the in vitro and in vivo studies accounts for functional redundancy between TGs due to high similarity in their substrate specificity (Achyuthan et al. 1996), and as a result, functional compensation for loss of each isoform by other TGs in embryonic development. Thus, compensatory activation of FXIIIa has been detected in the TG2^{-/-} chondrocytes (Nurminskaya and Kaartinen 2006; Tarantino et al. 2008), while TG5, TG1 and TG7 have been postulated to compensate for the loss of TG2 in other tissues (Grenard et al. 2001; Johnson et al. 2008).

To overcome complications associated with this compensation mechanism in the genetic loss-of-function mammalian models and to obtain insight into the role of TG-mediated cross-linking in bone formation, we employed the in vivo analysis of bone development in zebrafish (*Danio rerio*). Several physiologic features, such as early transparency, short maturation period, and high reproductive capacity, make this model ideal for studying developmental processes (Brittijn et al. 2009). Numerous developmental mechanisms in zebrafish, including bone development, share common factors with mammalian systems. In addition, the presence of orthologues for genes commonly seen in human diseases makes zebrafish especially useful for preliminary in vivo drug studies (Brittijn et al. 2009). Transglutaminase family has not been studied in zebrafish on either genetic or functional levels. In the present study, we analyzed the zebrafish genome for TG (zTGs) genes, and have identified 13 isoforms 11 of which are highly similar to one of the three human TGs (FXIIIa, TG2 and TG1). Taking into consideration that two of these mammalian homologues have been implicated in the regulation of mammal tissue calcification, we analyzed regulation of bone formation in zebrafish in which total TG activity was inhibited during vertebrae mineralization. Our study demonstrates a crucial role for TG-mediated cross-linking in bone calcification.

Materials and methods

BLAST search, sequence alignments and phylogenetic analysis

NCBI database of *D. rerio* protein sequences was searched with the blastp algorithm using the NCBI Blast server. We aligned the sequences with CLUSTAL-W (<http://www.ebi.ac.uk/Tools/clustalw2>) and constructed a phylogenetic tree using maximum parsimony algorithm with protpars tool in the PHYLIP 3.5 package (<http://www.es.emblnet.org>). We also aligned sequences and constructed a phylogenetic tree using the COBALT tool at NCBI (<http://www.ncbi.nlm.nih.gov/tools/cobalt>). Further, we used the phylogeny.fr package (<http://www.phylogeny.fr/version2.cgi/index.cgi>) for alignment and phylogenetic analyses.

Embryo generation and maintenance

Wild type zebrafish were maintained at the zebrafish facility of the Aquaculture Research Center, Center of Marine Biotechnology University of Maryland, as previously described (Du et al. 2001). Embryos were obtained from natural mating, staged according to morphology or by days post-fertilization (dpf), and kept at 28.5°C on a 14-h light 10-h dark cycle. During inhibitor treatment the zebrafish larvae were kept in six-well plates with five fish in 5 ml of water per well. Inhibitors were dissolved to a stock concentration of 10 mM in 100% Dimethyl Sulfoxide (DMSO) (Sigma, MO) and added directly to the fish water to a final concentration of 30 µM. Fish water, supplemented with paramisol and inhibitor, was changed once per day.

Ex vivo identification of TG cross-linking activity in zebrafish

Transglutaminase cross-linking activity in zebrafish was visualized ex vivo by incorporation of 5 mM rhodamine-conjugated synthetic substrate Pro-Val-Lys-Gly (SY2011) (Kim et al. 1997). Following the 4-h incubation at 28°C. Zebrafish were then washed with PBS and left overnight, to allow all unincorporated substrate to diffuse out, at room temperature in PBS. Zebrafish were then fixed in 4% PFA at room temperature for 2 h. Images were acquired by a Leica DMIL FLUO microscope equipped with a SPOT RT slider real-time CCD camera (Diagnostic Instruments, Inc.).

Whole mount in situ hybridization

Whole mount in situ hybridization was adapted from the previously described protocol (Thisse and Thisse 2007).

Embryos were fixed in 4% PFA and bleached with 3% hydrogen peroxide in 0.5% potassium hydroxide in PBS-T for 15 min. This was followed by Proteinase K (Novagen) digestion (10 µg/ml) for 30 min, second fixation in 4% PFA and acetone treatment for 8 min at -20°C . The DIG-labeled antisense RNA probes were used at 2 ng/µl concentration in the hybridization buffer. Hybridized DIG-RNA probes were detected with an anti-DIG fab fragments antibody fused to alkaline phosphatase (Roche, CA) at a 1:4,000 dilution followed by colorimetric assay with NBT/BCIP solution (Roche, CA) in the dark for 24–72 h until color developed. Staining progression was monitored with Nikon AZ100 microscope and analyzed with Nikon Elements software.

Real-time PCR

Total RNA was isolated from unfertilized eggs, 4, 13 dpf and torso of adult zebrafish with Trizol reagent (Invitrogen) and used for first-strand cDNA synthesis. Primers for zTGs were designed using NCBI primer design software (Table 1). The real-time PCR was run on a Roche Light-Cycler 480 II following the manufactures instructions for heat activation, amplification and melting curves for 45 cycles. Expression levels were normalized to β -actin mRNA.

TG activity assay

Total TG cross-linking activity in whole fish lysates was assayed by incorporation of the biotinylated pentylamine Ez-link Pentylamine-Biotin (Pierce, IL) into *N,N'*-Dimethylcasein (Sigma-Aldrich) in the ELISA-like assay as previously described (Trigwell et al. 2004). The 96-well microtiter plates (Maxisorp NUNC, UK) were incubated

overnight with 250 µl of 1 mg/ml *N,N'*-Dimethylcasein (Sigma-Aldrich) in 5 mM sodium carbonate (pH 9.8), and blocked with 200 µL of 0.1% bovine serum albumin (BSA) (HyClone, Ut) in 5 mM sodium carbonate (pH 9.8) for 1 h at 37°C . Whole 14 dpf zebrafish mated larvae were lysed in 5 mM Tris-HCl pH 7.5, 0.25 M Sucrose, 0.2 mM MgSO_4 , 2 mM DTT, 0.4 mM PMSF, 5 µg/ml leupeptine and 0.4% Triton X-100 (lysis buffer), centrifuged and TG-containing supernatant was used for further assays. Purified guinea pig liver transglutaminase 2 (gplTG2) (Sigma-Aldrich) was used as a standard for activity tests. For inhibitory studies, zebrafish lysates (20 ng total protein) or purified gplTG2 (75 ng purified protein) were pre-incubated with 100 µM inhibitors for one hour at 28°C . Reaction was carried out in 100 mM Tris-HCl pH 8.5, 6.7 mM CaCl_2 , 13.3 mM DTT and 2.5 mM Ez-link Pentylamine-Biotin (Pierce) for 1 h at 37°C . Incorporated Ez-link Pentylamine-Biotin was detected with 1:5,000 ExtrAvidin-Peroxidase (Sigma) and Super AquaBlue ELISA Substrate (eBioscience, CA) followed by reading the absorbance at 405 nm on a Polarstar Optima plate reader.

Calcein Staining of mineralized vertebrae

Protocol was adapted from Du et al. 2001. Zebrafish were transferred from fish water to 0.2% Calcein Stain (Sigma) in water, pH 7, and incubated in the dark for 10 min at room temperature. Fish were washed in ocean salt water (0.3 g/L aquarium salt) and then transferred into ocean salt water and incubated for 10 min in the dark at room temperature. After incubation zebrafish were euthanized with 0.4% Tricaine (Sigma), 20 mM Tris pH 9.0 and mounted in 3% methyl-cellulose. Images of the fluorescently stained vertebrae were taken 5 min after staining to avoid bleaching. Photos were taken with a Leica DMIL FLUO

Table 1 Primers used for real-time PCR analysis and accession numbers for zTGs

Target transglutaminase	Forward primer (5' → 3')	Reverse primer (5' → 3')	Accession number
zFXIIIa-87	GTTCGGCCCAACAGCGGGT	CCTGCGGATGCCGTACGGTG	NM_001077154
zTG2c	ACGCATCTGAACGGTGTGGACA	AAGGCAGATGTCCAGTATTCCGTGC	NM_001004647
zTG2b	GGCAAGTGATCCAACGCCGC	GGCGTCTCTGGTGCTGTAGTCGA	NM_212656
zTG-91	TGCTGATGACGGACGGGTCC	GATCCTCTGTCCCGGGCCGA	<u>XP_688146.5</u>
zTG-84	TGAACGCAGACGTGCGGACC	TGGCGCCCGTCATCTGAGGA	XM_689249
zTG1-81	ATCGCGGTGGAAACGGCCTG	CGCAGAGTGCAGGGCAGAGG	XM_689858
zTG1-48	CTCCGGAGCAAGAACTGCGAA	CTGTAGCGTCCGATGCACGC	XM_001331878
zTG1-96	TCATGCCTTTCTCATGCAGCCCA	CAGTGCGTCACAACGCTGAGC	XM_001332039
zTG1-73	ATATCCATCGAACTGAAGCTA	AGCCTTCAACTCTTTACCAAC	XP_002665624
zFXIIIa-53	ATCAATCTCCAATTCCCGAAC	TCCATCAAGGCGAAGCTCA	XP_686649
zFXIIIa-42	GAATTTAAAGCGACAGTCACC	TGAGCATTAAGCCATACACA	NP_001070179
zTG1-18	AGCACGTCAAAACCATCCAC	AGCACCTCCAAAATCAGATCG	XP_003201279
zTG2-12	AAGCCTCTGTCATTGTTTCG	GCTGTCATTGAGTATATCGC	XP_687398.2

microscope equipped with a SPOT RT slider real-time CCD camera (Diagnostic Instruments, Inc.). Intensity of the calcein staining was analyzed for each vertebra with Photoshop.

Data and statistical analysis

Data were collected and analyzed by both Microsoft Excel and Photoshop. Statistical significance was calculated by the student's *t* test and the error bars demonstrate the standard error mean.

Results

Identification of zebrafish TG Genes

To identify zebrafish TG genes (zTGs), we analyzed the current version of the NCBI zebrafish proteome database with blastp searches. By using human TG1, TG2, TG4, and FXIIIa protein sequences as queries, in each case we found the same set of fourteen homologous zebrafish proteins. Among these, one protein and corresponding gene LOC793095 initially described as a partial TG-homologous sequence has been removed from the genome assembly as not supported by sufficient evidence. Consistent with this, we did not detect expression of this gene through zebrafish development by real-time PCR. Therefore, our analysis identified 13 zTGs (Table 2). To further clarify phylogenetic relationship between the identified zTGs and human TGs, we performed multiple alignments of protein sequences and constructed phylogenetic trees using the following approaches: (i) TGs sequences were aligned with CLUSTAL-W and a phylogenetic tree was constructed using maximum parsimony algorithm with protpars tool in the PHYLIP 3.5 package, additionally (ii) sequence alignment and phylogenetic tree construction were done using the COBALT tool at NCBI, and (iii) phylogeny.fr package was used to align the sequences using the MUSCLE tool and to employ the maximum likelihood or neighbor-joining algorithm to construct the trees and analyze them with bootstrapping (1,000 iterations), or alternatively to use the Bayesian tree building algorithm with 1,000 iterations and burnin parameter of 50. All of these approaches resulted in the same tree configuration (a representative example of Bayesian tree is shown on Fig. 1a). We found that five zTGs (LOC's 793448, 100535918, 555962, 100334173, and 566581) are strikingly close to each other and to the human TG1 and probably originated by gene amplification after divergence of their common ancestor from the human TG1 (Fig. 1a). Also, three zTGs (LOC's 558353, 767742, and 561287) are similar to each other and to the human FXIIIa, and this group of zebrafish

Table 2 Zebrafish TG gene ID numbers and corresponding abbreviations used throughout the text

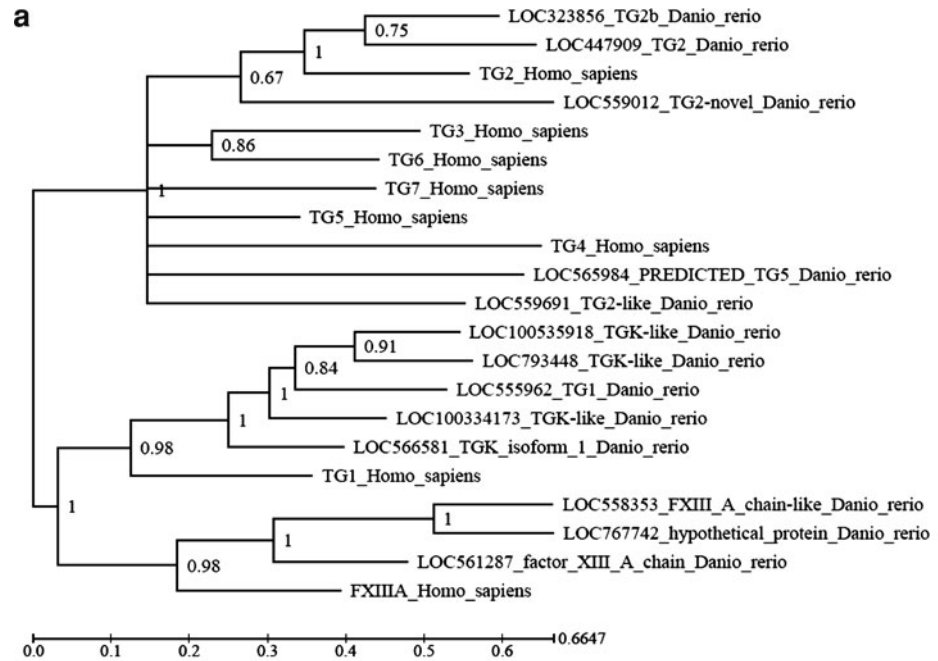
Gene name	Gene abbreviation
LOC555962 TG1	zTG1-62
LOC793448 TGK-like	zTG1-48
LOC100535918 TGK-like	zTG1-18
LOC566581 TGK isoform 1	zTG1-81
LOC100334173 TGK-like	zTG1-73
LOC323856 TG2b	zTG2b
LOC559012 TG2-novel	zTG2-12
LOC447909 TG2	zTG2c
LOC767742 hypothetical protein	zFXIIIa-42
LOC558353 FXIIIa chain-like	zFXIIIa-53
LOC561287 Factor XIII A chain	zFXIIIa-87
LOC559691 TG2-like	zTG-91
LOC565984 PREDICTED TG5	zTG-84

TGs also originated by a relatively recent gene amplification after their common ancestor diverged from the human FXIIIa. Further, three zTGs are similar to human TG2. Among these, two genes (LOC's 323856 and 447909) originated after their common ancestor split from human TG2, and another one (LOC559012) is more ancient. Finally, two zebrafish TGs have been annotated as TG2-like (LOC559691) and TG5 (LOC565984). However, these zebrafish proteins are similarly distant from all human TGs based on pairwise comparisons (Fig. 1b) and their association with human homologs suggested by annotations, or with other human TGs, is not well supported by phylogenetic analysis. Therefore, based on the sequence analysis these two zTGs should be considered as novel TG isoforms, and we refer to these henceforth as zTG-91 and zTG-84 (Table 2).

Chromosomal arrangement of the zTG genes (Fig. 2a; schematic diagram of the chromosomal arrangements of TG genes in human and zebrafish genomes is shown in Fig. 2b) is dramatically different from the TGs gene clustering pattern in humans (Grenard et al. 2001) where TG2, TG3, and TG6 form a cluster on chromosome 20, TG5 and TG7 are clustered on chromosome 15, and TG1, TG4, and FXIIIa are present on different chromosomes. In zebrafish, the TG1/TGK-like transglutaminase genes are located on two chromosomes. The most ancient gene zTG1-81 (LOC566581) is located on chromosome 2, and the other four genes are located on chromosome 23. Among these, the two most recently diverged genes zTG1-18 (LOC100535918) and zTG1-48 (LOC793448) are separated by 1 Mb, and the others are located more distantly (Fig. 2a, b). A similar arrangement exists for the FXIIIa-like transglutaminases, where the most ancient gene LOC561287 is located on chromosome 7 and the two

Fig. 1 Phylogenetic analysis of TG genes in zebrafish.

a Phylogenetic tree depicting the evolutionary relationships among TG genes of *Danio rerio* and human origin as established by the Bayesian tree building algorithm. Only three out of nine mammalian TGs have an overt zebrafish homologue, including *TG2*, *FXIIIa* and *TG1*. **b** Table showing low similarity between the two novel zTGs, LOC559691 TG2-like and LOC565984 TG5, and diverse human TGs



b

Percent Similarity Between Human and Zebrafish TGs								
	hTG1	hTG2	hTG3	hTG4	hTG5	hTG6	hTG7	hFXIII
LOC559691 TG2-like	53	57	56	54	55	58	54	52
LOC565984 TG5	52	54	54	51	57	54	52	52

recently diverged genes LOC558353 and LOC767742 are both located on chromosome 24 separated by a mere 7 kb. In contrast, all three zTG2 genes are located on different chromosomes with the most ancient zTG2 genes (LOC559012) being located on chromosome 18, and LOC323856 on chromosome 6 versus LOC447909 on chromosome 23 despite their recent divergence. The remaining zebrafish TG genes that are not closely related to other TGs (LOC565984 and LOC559691) are located on the opposite ends of chromosome 6. All zTG genes have introns and hence are likely not the products of retrotranspositions. Thus, the expansion of the TG2-like subfamily and initial expansions of the TG1-like and FXIIIa-like subfamilies in zebrafish may have been associated with gene duplications and inter-chromosomal rearrangements, while further amplification of the FXIIIa-like and TG1-like genes probably occurred by local gene duplications which in the case of TG1-like genes were followed with intra-chromosomal rearrangements. These findings, and the absence of overt TG3, TG4, TG5, TG6 and TG7 homologs in zebrafish, raise a possibility that amplification of the human TG genes occurred after the evolutionary split

between these species. Accordingly, it appears that the expansion of the TG1-like, TG2-like, and FXIIIa-like gene families in zebrafish occurred independently during the same time period.

Expression and activity of TGs in zebrafish

The expression profiles for all identified zTG genes were analyzed by real-time PCR in both embryonic development stages and adult fish. Since our study aimed to determine the role of zTGs in bone calcification, which begins around 5 dpf and is completed by 16 dpf when calcification of all vertebrae can be visualized with vital calcein staining (Du et al. 2001), we analyzed expression of zTGs in the 4 dpf larvae just before the initiation of vertebral calcification, and in the 13 dpf larvae when most vertebrae have already been calcified. In addition, expression levels for zTG genes were analyzed in adult torso presenting homeostatic bone. Expression of each zTG was normalized to the house-keeping β -actin gene and compared to unfertilized eggs. This analysis identified five zebrafish TGs (zFXIII-87, zTG2c, zTG2-12, zTG1-81, and zTG1-73) induced in

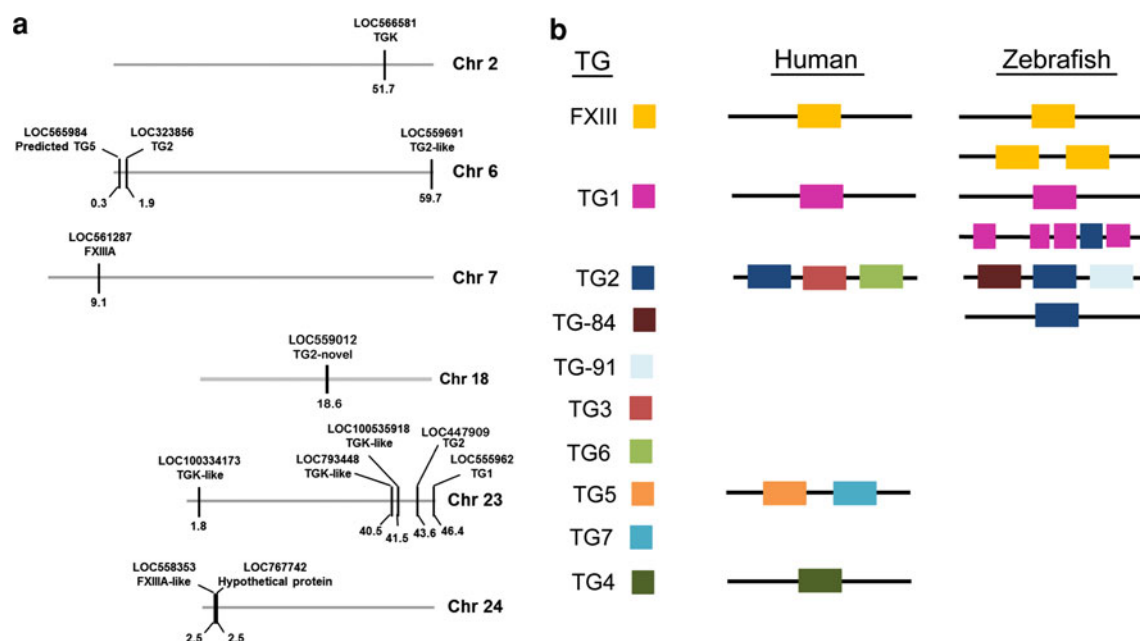


Fig. 2 Analysis of genomic organization of TG genes in zebrafish. **a** Chromosomal arrangement of zebrafish TG genes. **b** Color-coded schematic of chromosomal clustering of TGs in both human and zebrafish

larvae as compared to the non-fertilized eggs, but almost completely silenced in adulthood (Fig. 3a), implicating their involvement in the developmental processes. In contrast, zFXIIIa-53 and zFXIIIa-42 are both up-regulated in adult tissue (Fig. 3b), suggesting a putative role for these enzymes in body homeostasis rather than in growth and development. A minor role in fish growth and development is also suggested for two zTG1 genes—zTG1-62 and zTG1-18—based on their dramatic down-regulation after fertilization.

No expression was detected by the real-time PCR analysis for zTG1-48 at any stage (data not shown), implicating that this locus maybe a silent pseudogene, however, more detailed studies are required to test this further. Conversely, novel genes zTG-84 and zTG-91, in addition to zTG2b, are almost ubiquitously expressed in zebrafish tissues at all analyzed stages (Fig. 3b, zTG-84 is not included in the figure because all data in this figure is normalized to non-fertilized eggs in which zTG-84 is not expressed), resembling the ubiquitous expression of mammalian TG2 enzyme. The most noticeable distinction between these three ubiquitous zTGs is the complete absence of zTG-84 transcript in the non-fertilized eggs, suggesting its reduced role in early embryogenesis.

Localization of zTG expression by in situ hybridization

The expression data from the real-time PCR analysis was expanded by in situ hybridization studies on the 2–3 dpf zebrafish. Although many zTGs were not detectable at

these stages by in situ hybridization indicating relatively low levels of expression, expression of several genes was observed in a tissue-specific pattern (Fig. 4a, top panel). Thus, zTG2c expression is restricted to muscles while zTG1-81 is expressed in the muscle and, likely, in the notochord. Expression of zTG2b is restricted to notochord and zFXIIIa-87 is detected in the pectoral fin. Sense RNA probes were used as negative controls (Fig. 4a, low panel). The identified muscle-specific expression of zTG1-81 and zTG2c in 2–3 dpf fish suggests a role for these enzymes in muscle development. While zTG2c has been detected in the muscle even earlier, at 1 dpf fish [ZFIN (<http://zfin.org/cgi-bin/webdriver?Mval=aa-xpatslect.apg>)], further analysis is needed to investigate in more detail the stage-specific and muscle-type-specific expression of zTG1-81. A novel finding of our study is the notochord-specific expression of zTG2b in the 2–3 dpf fish. Earlier in development, at 1 dpf, this gene is ubiquitously expressed throughout the embryo [ZFIN (<http://zfin.org/cgi-bin/webdriver?Mval=aa-xpatslect.apg>)], suggesting that it may be expressed in the progenitor cells which give rise to the osteo-chondrogenic lineage. This pattern of expression corresponds to that seen for the TG2 gene in avian mesenchymal limb bud cells (Nurminsky et al. 2010) and suggests a role for this enzyme in skeletal formation. In addition, expression of zFXIIIa-87 was detected in the developing fins, which are enriched with skeletal ray elements, implicating this enzyme in bone formation. To determine whether zTGs expressed in the skeletal and muscle tissue are enzymatically active, we employed a rhodamine-labeled peptide

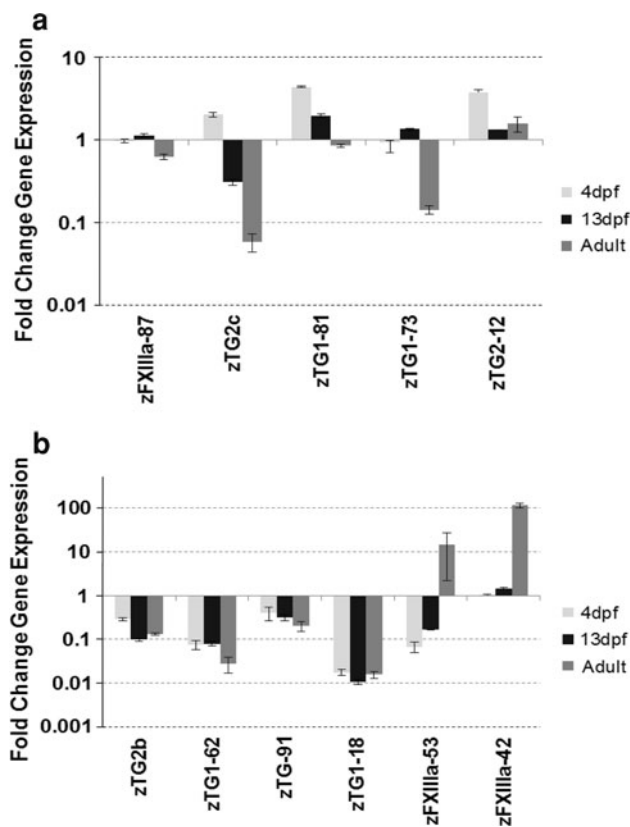


Fig. 3 Expression patterns of TGs during zebrafish development. Real-time PCR analysis was used to determine TGs expression pattern. Whole bodies were used for analysis at 4, 13 dpf and the torso from adult zebrafish. Data were normalized to β -actin and compared to unfertilized eggs. **a** Real-time PCR showing TG genes that are upregulated during development (in 4 and 13 dpf zebrafish). **b** Real-time PCR analysis showing the TG genes that have either little change in expression during development or significant upregulation in adult fish

Pro-Val-Lys-Gly, also called SY2011, which is a substrate for TGs (Kim et al. 1997). Decapitated fish were incubated with 5 mM Rho-SY2011 for ex vivo incorporation through TG-mediated cross-linking. Incorporated peptide was visualized by rhodamine fluorescence (Fig. 4b) to detect tissue with active zTGs. In agreement with the results of in situ hybridization, SY2011 was cross-linked into striated muscles of the torso, into periosteal bone of the vertebrae and in the in large blood vessels.

Together, these results demonstrate presence of the enzymatically active TGs in the developing skeleton of zebrafish justifying this organism as a good model to analyze the role of TGs in bone formation.

KCC009 is a potent inhibitor of TGase cross-linking activity in zebrafish tissues

To analyze the role for the TG-mediated cross-linking in bone formation, we employed a pharmacologic approach to

inhibit total catalytic activity of TGs with a small molecule inhibitor KCC-009 which inhibits the deamidation step of the cross-linking reaction (Poster et al. 1981; Choi et al. 2005). Using pentylamine-based activity assay, we tested the potency of KCC-009 in inhibiting total TG cross-linking activity in total tissue lysates from 19 dpf zebrafish. Purified guinea pig liver TG2 was used as a control in these studies, which demonstrated the complete inhibition of the TG-mediated cross-linking in zebrafish tissues (Fig. 5a). We also found that KCC-009 was able to inhibit protein cross-linking in adult tissue extracts (data not shown), indicating that it can be used to study the role of TGs both in fish development and in adult tissue homeostasis.

In vivo, KCC-009 showed low toxicity in mice and cancer xenografts (Choi et al. 2005; Yuan et al. 2007; Satpathy et al. 2009). Similarly, KCC-009 had no toxic effects on zebrafish as evident by unaffected viability (Fig. 5b), standard length (SL) as a reflection of development (Parichy et al. 2009) (Fig. 5c) and total vertebrae number (Fig. 5d) in zebrafish treated with 30 μ M KCC-009 for 5–6 days when treatment was initiated before 6 dpf (Fig. 5). Moreover, when KCC-009 treatment was started at 4 dpf, we observed a slight but significant increase in vertebrae number from an average of 18 vertebrae in control fish up to 21 vertebrae in the KCC-009 treated animals (Fig. 5d) ($p < 0.05$, $n = 9$).

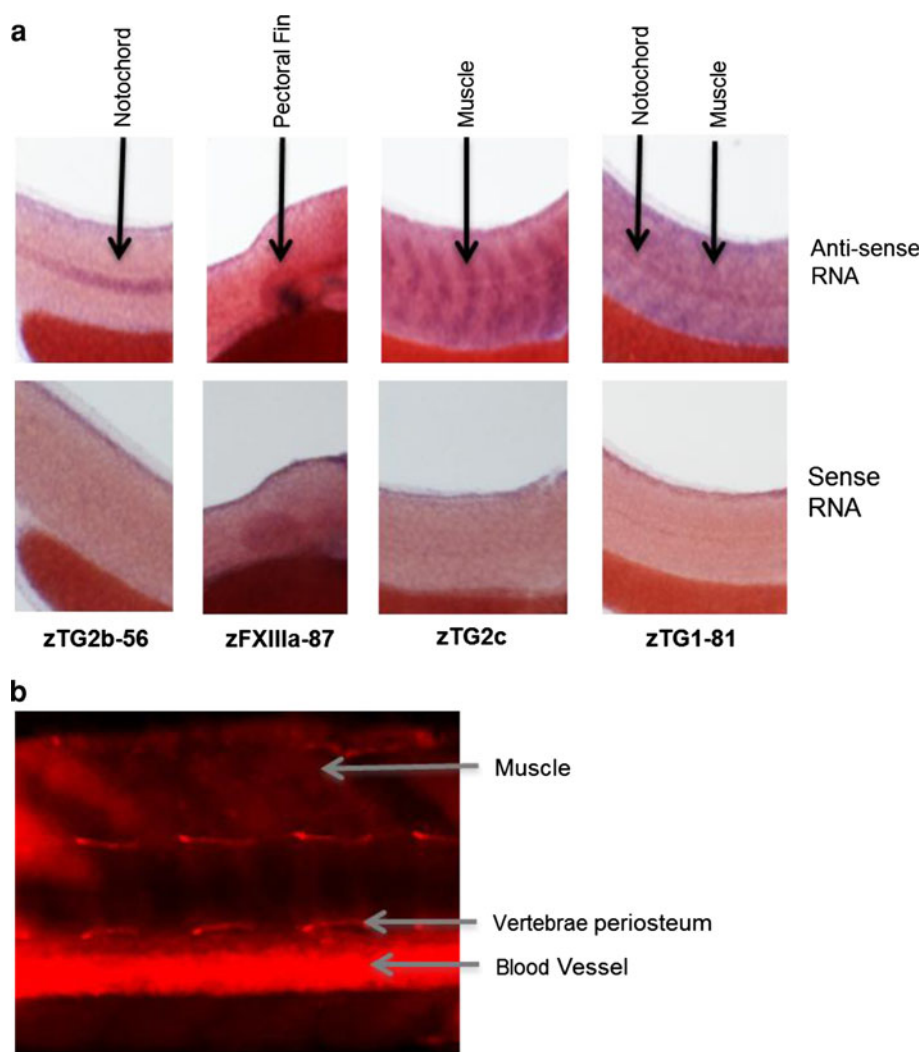
In vivo inhibition of TG activity with KCC-009 affects bone formation

In order to analyze the role of TGs in bone formation, we grew zebrafish in the continuous presence of 30 μ M KCC-009 over 5 days starting at 3–5 dpf. Control fish were grown in the presence of 0.3% DMSO which served as the vehicle for KCC-009. Bone mineralization was analyzed by in vivo calcein staining (Du et al. 2001). A representative pair of calcein stained vertebrae for both the control and KCC-009 treated zebrafish is shown in Fig. 6a, demonstrating the dramatic decrease in vertebrae mineralization for the KCC-009 treated group. Quantitative analysis of calcein staining intensity of the mineralized vertebrae revealed a significant average decrease of 30% in mineralization for the KCC-009-treated fish (Fig. 6b; $p < 0.05$, $n = 45$), although there was a high variation in the degree of KCC-009 induced reduction in vertebrae calcification. Due to KCC-009's potent ability to inhibit the cross-linking activity of all zTGs (Fig. 5a), these results suggest that TG-mediated cross-linking plays a critical role in vertebrae ossification.

Discussion

In this study, we have characterized the new family of TG genes in zebrafish, *D. rerio*. Thirteen zebrafish TG genes

Fig. 4 Tissue specific expression of TGs in 2–3 dpf zebrafish. **a** Representative images from whole mount in situ hybridization for zTG2b, zFXIII, zTG2c and zTG1-81 showing the tissue-specific expression patterns for TGs (*top*) and the negative control hybridization with the sense probes (*bottom*). **(b)** Ex vivo incorporation of the rhodamine-labeled synthetic substrate Pro-Val-Lys-Gly in zebrafish showing areas with high TG cross-linking activity in the ossifying vertebrae, blood vessels and muscle



homologous to mammalian TGs have been identified, of which five are homologous to human TG1 (hTG1), three are homologues of hTG2 and three show homology to hFXIIIa, as revealed by phylogenetic analysis. Two zebrafish TGs show little similarity to any of the human TGs and have therefore been classified as novel TGs with the names zTG-84 and zTG-91, in spite of previous annotations for these genes as homologues of hTG5 and hTG2.

Expression pattern of the zTGs analyzed at 4, 13 dpf and in adult fish by real-time PCR shows ubiquitous expression of zTG-84, zTG-91 and zTG2b genes, resembling the ubiquitous expression of mammalian TG2 enzyme, which is implicated in many biological processes including bone formation. In addition, zFXIIIa-87, zTG2c, zTG1-81, zTG1-73 and zTG2-12 are up-regulated during stages of development that are significant to bone mineralization, implicating their potential role in bone development. Our data from in situ hybridization further supports this hypothesis by demonstrating the notochord-specific expression of zTgb, restricted expression of zFXIIIa-87 to

the pectoral fins and presence of zTG1-81 RNA in the notochord. In contrast, mRNA for zTGc was identified only in skeletal muscle in agreement with earlier studies (Thisse et al. 2004) and supporting specificity of this analysis. Although RNAs for several zTGs were not detected by in situ hybridization in this study, likely due to low levels of their expression, the data obtained clearly demonstrates expression of TG2 and FXIIIa genes in the skeletal tissues. Mammalian homologues of these genes have been implicated as potent regulators of osteoblast differentiation in vitro (Nurminskaya et al. 2003; Becker et al. 2008), supporting a notion that TGs may also regulate bone development in vivo.

The original finding of this study is the demonstrated reduction in vertebrae calcification in zebrafish grown in the presence of TG-specific irreversible acivicin-derived inhibitor KCC-009. No signs of general toxicity of KCC-009 were observed in zebrafish grown from 3 to 4 dpf until 9 to 10 dpf in its presence, suggesting that tissue-specific inhibition of TG-mediated cross-linking in the skeleton

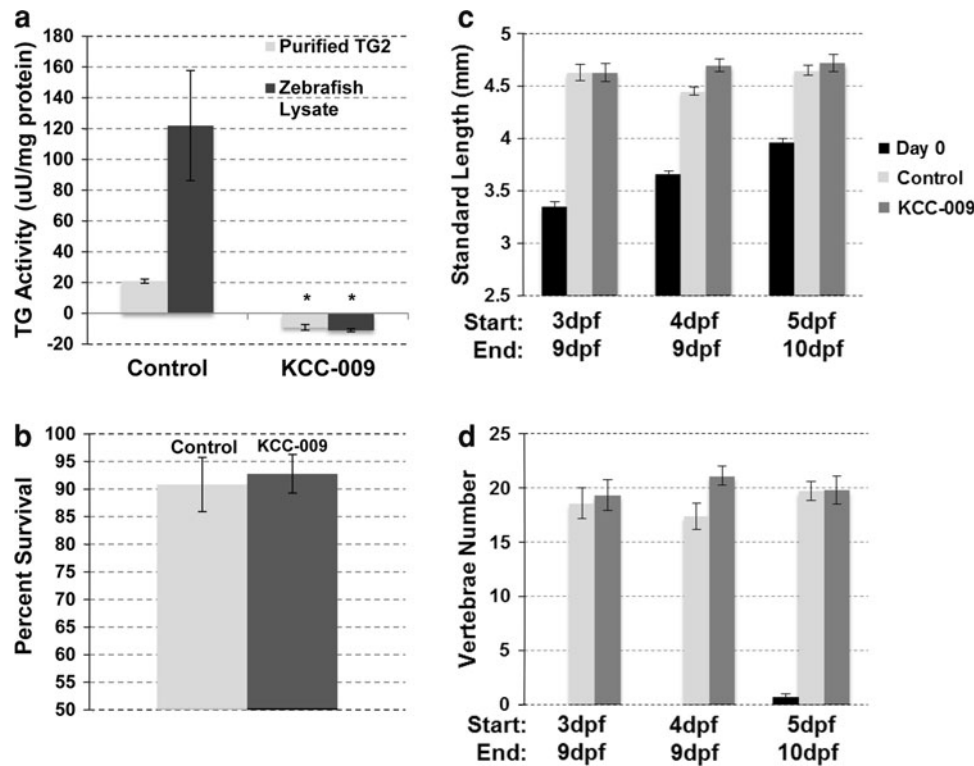


Fig. 5 KCC-009 is a potent inhibitor of total cross-linking TG activity in vitro and has no toxic effects in zebrafish. **a** TG cross-linking activity assayed by pentylamine-biotin incorporation into *N,N'*-dimethylcasein. Total protein lysates from 14 dpf zebrafish were used. To inhibit TG activity samples were pre-incubated for 1 h at 28°C with KCC-009. Purified guinea pig liver TG2 (Sigma) was used as positive control (* $P \leq 0.05$). Toxicity of KCC-009 treatment was

analyzed by comparing the **(b)** average survival percent, **(c)** standard length in millimeters and **(d)** average total vertebrae number (Day 0 black bar, control at 9/10 dpf light grey bar and KCC-009 treated at 9/10 dpf dark grey bar in **c** and **d**) for the untreated control zebrafish and fish grown for 5–6 days in the presence of 30 μ M KCC-009. $N = 9$ –16 per time point (* $P \leq 0.05$)

underlies this effect. Our initial in situ analysis on 2–3 dpf fish has identified expression of three zTG genes in the skeletal tissues, including zTG2b, zFXIIIa-87 and zTG1081. However, other zTGs may be also expressed in the mineralizing bone later in development, and this should be studied in more detail for comprehensive understanding of the molecular control of tissue calcification. Although the demonstrated importance of TG activity in vertebrae mineralization is an important contribution towards this goal, the weak selectivity of KCC-009 toward individual zTGs is a limitation of this study. The KCC-009 compound efficiently inhibits total TG activity in the zebrafish lysates in which expression of at least nine isogenes have been identified at each analyzed stage of growth. This precludes identification of the roles of individual zTGs in the regulation of bone calcification. In the future, we plan to generate transgenic fish to establish the roles of individual enzymes in bone mineralization, taking into consideration previous in vitro studies which have implicated a major role for FXIIIa (Nurminskaya et al. 1998; Nakano et al. 2007).

Although the precise mechanism of TG-dependent bone calcification remains to be determined, a credible model

would account for the formation of cross-linked protein scaffolds, such as a collagen type 1-fibronectin cross-linked network, which has previously been shown to promote matrix mineralization in the MC3T3-E1 osteoblastic cell line (Al-Jallad et al. 2005). A peak in collagen type 1 expression around 2–3 dpf in growing zebrafish (Dubois et al. 2002) could allow for formation of such a scaffold in the vertebrae. This scaffold would then be susceptible to calcification which culminates in visually detectable levels of calcium deposited into vertebrae beginning at 5 dpf (Du et al. 2001). Inhibition of the TG-dependent cross-linking starting at 3 dpf interferes with this process thereby inhibiting vertebrae calcification.

Comprehensive understanding of the molecular mechanisms that govern osteoblast maturation and calcification of bone matrix is crucial to develop novel therapeutics for bone disease. Bone tissue homeostasis requires a delicate balance between bone formation by osteoblasts and bone resorption by osteoclasts, which is disrupted in osteoporosis. The current approach to treatment for osteoporosis relies on anti-resorptive agents to inhibit osteoclast function but do not restore bone mass (Rawadi 2008). This

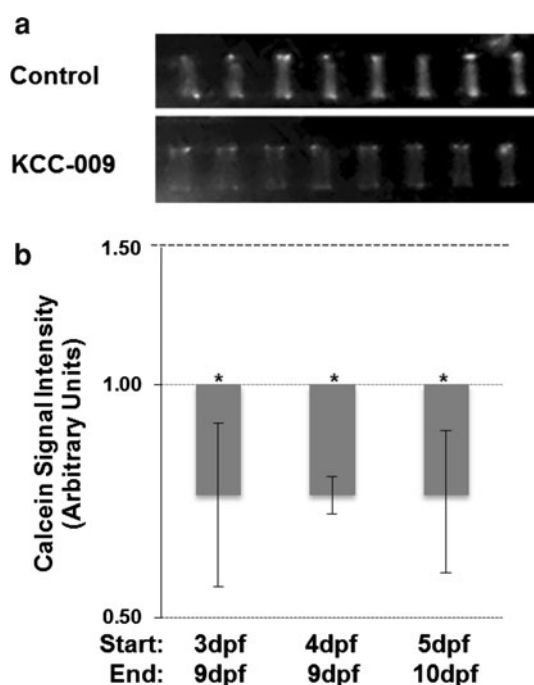


Fig. 6 Inhibition of TGs by KCC-009 dramatically reduces vertebrae mineralization. Zebrafish were grown for 5–6 days starting at 3–5 dpf in the presence of KCC-009. **a** Representative calcein stained images of zebrafish, Control (*top*) and KCC-009 (*bottom*) treated fish, KCC-009 treatment started at 3 dpf and images taken at 9 dpf, shown in greyscale. **b** Average change in calcein staining intensity per vertebra in the presence of KCC-009. Intensity of calcein staining for each vertebra was determined with Photoshop. $N = 16$ fish for 5 dpf treatment, 9 for 4 dpf treatment and 20 for 3 dpf experiment (* $P \leq 0.05$)

study provides the first in vivo evidence for the critical role of TG-mediated cross-linking in bone mineralization which could lead to a new therapeutic target in osteoporosis and other bone diseases. Furthermore, this study demonstrates the value of the zebrafish model for in vivo analysis of the multiple biological roles of transglutaminases proposed by the in vitro or correlative studies, including various developmental processes and disorders such as neurodegenerative, skin and ocular pathologies as well as cancer (Mione and Trede 2010).

Acknowledgments We would like to thank Dr. Dmitry Nurminsky for critical discussion concerning the genetic analysis of TGs in zebrafish, and Dr. Chaitan Khosla for providing us with the TG inhibitor KCC-009. We would also like to thank Dr. Elayne Provost and Dr. Steve D. Leach for their help in photographing and visualizing the whole mount in situ hybridization. This work was supported by NIH grants HL093305, AR057126 and DK071920, and support from Maryland Stem Cell Research Foundation to M. Nurminskaya.

References

Achyuthan KE, Rowland TC, Birckbichler PJ, Lee KN, Bishop PD, Achyuthan AM (1996) Hierarchies in the binding of human

factor XIII, factor XIIIa, and endothelial cell transglutaminase to human plasma fibrinogen, fibrin, and fibronectin. *Mol Cell Biochem* 162(1):43–49

Aeschlimann D, Wetterwald A, Fleisch H, Paulsson M (1993) Expression of tissue transglutaminase in skeletal tissues correlates with events of terminal differentiation of chondrocytes. *J Cell Biol* 120:1461–1470. doi:10.1083/jcb.120.6.1461

Al-Jallad HF, Nakano Y, Chen JLY, McMillan EK, Lefebvre C, Kaartinen MT (2005) Transglutaminase activity regulates osteoblast differentiation and matrix mineralization in MC3T3-E1 osteoblast cultures. *Matrix Biol* 25:135–148. doi:10.1003/jbmr.5650070613

Becker S, Maissen O, Ponomarev I, Stoll T, Meury T, Sprecher C, Alini M, Wilke I (2008) Osteopromotion with a plasmatransglutaminase on a beta-TCP ceramic. *J Mater Sci Mater Med* 19:659–665. doi:10.1007/s10856-007-3223-2

Bianco P, Cancedda FD, Riminucci M, Cancedda R (1998) Bone formation via cartilage models: the “borderline” chondrocyte. *Matrix Biol* 3:185–192. doi:10.1016/S0945-053X(98)90057-9

Borge L, Demignot S, Adolphe M (1996) Type II transglutaminase expression in rabbit articular chondrocytes in culture: relation with cell differentiation, cell growth, cell adhesion and apoptosis. *Biochim Biophys Acta* 312:117–124. doi:10.1016/0167-4889(96)00028-6

Brittijn SA, Duivesteyn SJ, Belmamoune M et al (2009) Zebrafish development and regeneration: new tools for biomedical research. *Int J Dev Biol* 53:835–850. doi:10.1387/jdb.082615sb

Choi K, Siegel M, Piper JL, Yuan L, Cho E, Strnad P, Omary B, Rich KM, Khosla C (2005) Chemistry and biology of dihydroisoxazole derivatives: selective inhibitors of human transglutaminase 2. *Chem Biol* 12:469–475. doi:10.1016/j.chembiol.2005.02.007

Du SJ, Frenkel V, Kindschi G, Zohar Y (2001) Visualizing normal and defective bone development in zebrafish embryos using the fluorescent chromophore calcein. *Dev Biol* 238:239–246. doi:10.1006/dbio.2001.0390

Dubois GM, Haftek Z, Crozet C, Garrone R, Guellec DL (2002) Structure and spatio temporal expression of the full length DNA complementary to RNA coding for $\alpha 2$ type I collagen of zebrafish. *Gene* 294:55–65. doi:10.1016/S0378-1119(02)00770-9

Faverman L, Mikhaylova L, Malmquist J, Nurminskaya M (2008) Extracellular transglutaminase 2 activates beta-catenin signaling in calcifying vascular smooth muscle cells. *FEBS Lett* 582:1552–1557. doi:10.1016/j.febslet.2008.03.053

Grenard P, Bates MK, Aeschlimann D (2001) Evolution of transglutaminase genes: identification of a transglutaminase gene cluster on human chromosome 15q15. *J Biol Chem* 276(35):33066–33078. doi:10.1074/jbc.M10255320

Johnson K, Hashimoto S, Lotz M, Pritzker K, Terkeltaub R (2001) Interleukin-1 induces pro-mineralizing activity of cartilage tissue transglutaminase and factor XIIIa. *Am J Pathol* 159:149–163. doi:10.1016/S0002-9440(10)6682-3

Kim SY, Park WM, Jung SW, Lee J (1997) Novel transglutaminase inhibitors reduce the cornified cell envelope formation. *Biochem Biophys Res Commun* 233:39–44. doi:10.1006/bbrc.1997.6407

Koseki-Kuno S, Yamakawa M, Dickneite G, Ichinose A (2003) Factor XIII A subunit-deficient mice developed severe uterine bleeding events and subsequent spontaneous miscarriages. *Blood* 102:4410–4412. doi:10.1182/blood-2003-05-1467

Lauer P, Metzner HJ, Zettlmeissl G, Li M, Smith AG, Lathe R, Dickneite G (2002) Targeted inactivation of the mouse locus encoding coagulation factor XIII-A: hemostatic abnormalities in mutant mice and characterization of the coagulation deficit. *Thromb Haemost* 88:967–974

Lorand L, Graham RM (2003) Transglutaminases: crosslinking enzymes with pleiotropic functions. *Nat Rev Mol Cell Biol* 4:140–156. doi:10.1038/nrm1014

- Mione MC, Trede NS (2010) The zebrafish as a model for cancer. *Dis Model Mech* 3:517–523. doi:[10.1242/dmm.004747](https://doi.org/10.1242/dmm.004747)
- Nakano Y, Al-Jallad HF, Mousa A, Kaartinen MT (2007) Expression and localization of plasma transglutaminase factor XIIIa in bone. *J Histochem Cytochem* 55:675–685. doi:[10.1369/jhc.6A7091.2007](https://doi.org/10.1369/jhc.6A7091.2007)
- Nanda N, Iismaa SE, Owens WA, Husain A, Mackay F, Graham RM (2001) Targeted inactivation of Gh/tissue transglutaminase II. *J Biol Chem* 276:20673–20678. doi:[10.1074/jbc.M010846200](https://doi.org/10.1074/jbc.M010846200)
- Nurminskaya M, Kaartinen MT (2006) Transglutaminases in mineralized tissues. *Front Biosci* 11:1591–1606. doi:[10.2741/1907](https://doi.org/10.2741/1907)
- Nurminskaya M, Linsenmayer TF (1996) Identification and characterization of up-regulated genes during chondrocyte hypertrophy. *Dev Dyn* 206:260–271. doi:[10.1002/\(SICI\)1097-0177\(199607\)206:3<260::AID-AJA4>3.0.CO;2-G](https://doi.org/10.1002/(SICI)1097-0177(199607)206:3<260::AID-AJA4>3.0.CO;2-G)
- Nurminskaya MV, Linsenmayer TF (2002) Immunohistological analysis of transglutaminase factor XIIIa expression in mouse embryonic growth plate. *J Orthop Res* 20(3):575–578. <http://www.ncbi.nlm.nih.gov/pubmed/12038633>
- Nurminskaya M, Magee C, Nurminsky D, Linsenmayer TF (1998) Plasma transglutaminase in hypertrophic chondrocytes: expression and cell-specific intracellular activation produce cell death and externalization. *J Cell Biol* 142(4):1135–1144. doi:[10.1083/jcb.142.4.1135](https://doi.org/10.1083/jcb.142.4.1135)
- Nurminskaya MV, Recheis B, Nimpf J, Magee C, Linsenmayer TF (2002) Transglutaminase factor XIIIa in the cartilage of developing avian long bones. *Dev Dyn* 233:24–32. doi:[10.1002/dvdy.1230](https://doi.org/10.1002/dvdy.1230)
- Nurminskaya M, Magee C, Faverman L, Linsenmayer TF (2003) Chondrocyte-derived transglutaminase promotes maturation of preosteoblasts in periosteal bone. *Dev Biol* 263:139–152. doi:[10.1016/S0012-1606\(03\)00445-7](https://doi.org/10.1016/S0012-1606(03)00445-7)
- Nurminsky D, Shanmugasundaram S, Deasey S, Michaud C, Allen S, Hendig D, Dastjerdi A, Francis-West P, Nurminskaya M (2010) Transglutaminase 2 regulates early chondrogenesis and glycosaminoglycan synthesis. *Mech Dev* 128:234–245. doi:[10.1016/j.mod.2010.11.007](https://doi.org/10.1016/j.mod.2010.11.007)
- Parichy DM, Elizondo MR, Mills MG, Gordon TN, Engeszer RE (2009) Normal table of postembryonic zebrafish development: staging by externally visible anatomy of the living fish. *Dev Dyn* 238:2975–3015. doi:[10.1002/dvdy.22113](https://doi.org/10.1002/dvdy.22113)
- Poster DS, Bruno S, Penta J, Neil GL, McGovren JP (1981) Acivicin: an antitumor antibiotic. *Cancer Clin Trials* 4:327–330
- Rawadi G (2008) Wnt signaling and potential applications in bone diseases. *Curr Drug Targets* 9:581–590. doi:[10.2174/138945008784911778](https://doi.org/10.2174/138945008784911778)
- Rosenthal AK, Derfus BA, Henry LA (1997) Transglutaminase activity in aging articular chondrocytes and articular cartilage vesicles. *Arthritis Rheum* 40:966–970. doi:[10.1002/art.1780400526](https://doi.org/10.1002/art.1780400526)
- Satpathy M, Shao M, Emerson R, Donner D, Matei D (2009) Tissue transglutaminase regulates matrix metalloproteinase-2 in ovarian cancer by modulating camp-response element-binding protein activity. *J Biol Chem* 284:15390–15399. doi:[10.1074/jbc.M808331200](https://doi.org/10.1074/jbc.M808331200)
- Summey BT, Graff RD, Lai TS, Greenberg CS, Lee GM (2002) Tissue transglutaminase localization and activity regulation in the extracellular matrix of articular cartilage. *J Orthop Res* 20:76–82. doi:[10.1016/S0736-0266\(01\)00064-X](https://doi.org/10.1016/S0736-0266(01)00064-X)
- Tarantino U, Oliva F, Taurisano G, Orlandi A, Pietroni V, Candi E, Melino G, Maffulli N (2008) FXIIIa and TGF-beta overexpression produces normal musculo-skeletal phenotype in TG2^{-/-} mice. *Amino Acids* 36:679–684. doi:[10.1007/s00726-008-0133-7](https://doi.org/10.1007/s00726-008-0133-7)
- Thisse C, Thisse B (2007) High-resolution in situ hybridization to whole-mount zebrafish embryos. *Nat Protoc* 3:59–69. doi:[10.1038/nprot.2007.514](https://doi.org/10.1038/nprot.2007.514)
- Thisse B, Heyer V, Lux A, Alunni V, Degraeve A, Seiliez I, Kirchner J, Parkhill JP, Thisse C (2004) Spatial and temporal expression of the zebrafish genome by large-scale in situ hybridization screening. *Methods Cell Biol* 77:505–519. doi:[10.1016/S0091-679X\(04\)77027-2](https://doi.org/10.1016/S0091-679X(04)77027-2)
- Trigwell SM, Lynch PT, Griffin M, Hargreaves AJ, Bonner PL (2004) An improved colorimetric assay for the measurement of transglutaminase (type II)–(gamma-gltamyl) lysine cross-linking activity. *Anal Biochem* 330:164–166. doi:[10.1016/j.ab.2004.03.068](https://doi.org/10.1016/j.ab.2004.03.068)
- Yuan L, Siegel M, Choi K, Khosla C, Miller CR, Jackson EN, Piwnicka-Worms D, Rich KM (2007) Transglutaminase 2 inhibitor, KCC009, disrupts fibronectin assembly in the extracellular matrix and sensitizes orthotopic glioblastomas to chemotherapy. *Oncogene* 26:2563–2573. doi:[10.1038/sj.onc.1210048](https://doi.org/10.1038/sj.onc.1210048)